ELSEVIER

International Journal of Heat and Fluid Flow 19 (1998) 125–134

International Journal of
HEAT AND
FLUID FLOW

Progress in direct numerical simulation of turbulent transport and its control

Nobuhide Kasagi [1]

Department of Mechanical Engineering, The University of Tokyo, Bunkyo-ku, Tokyo 113, Japan

Received 7 August 1997; accepted 25 October 1997

Abstract

With continuous advances in large scale computers, numerical methods and post-processing environment, direct numerical simulation (DNS) has played an important role in various fundamental studies of turbulent transport and its sophisticated control. After general remarks on grid requirement and numerical techniques of DNS, its novelty is highlighted through its recent applications to a dynamically complex flow and a flow control problem. The DNS of a channel flow under coupled dynamical effects of buoyant and Coriolis forces reveals peculiar phenomena of momentum and heat transfer with the quasi-coherent structures being strikingly altered. In a trial simulation of the active turbulence control with a virtual damping force, the most effective spatio-temporal distribution of the control input is sought by adopting a suboptimal control theory. Future directions of DNS for turbulence transport research are also discussed.

Keywords: Turbulent heat transfer; Direct numerical simulation; Rotation; Buoyancy; Control

1. Introduction

The turbulent momentum and scalar transport plays a key role in many engineering applications and will be of growing importance in global environmental problems. For instance, it is necessary to predict flow and heat transfer characteristics under design conditions, if one has to establish efficient and safe industrial systems such as aircrafts, ships, automobiles and power plants. Control of thermo-fluids phenomena in various equipment and production processes is crucial to keeping high quality, reliability and safe operation of products. Hence, much effort in fundamental turbulence research has been devoted to developing methodologies for prediction and control of various turbulent flows and associated transport phenomena. In the early 1980s, with the advancement of large scale computers, direct numerical simulation (DNS, hereafter) of turbulent shear flows had become possible. In particular, since the DNSs of the flows of engineering importance such as turbulent channel flows with heat transfer were carried out by, e.g., Moser and Moin (1987), Kim et al. (1987) and Kim and Moin (1989), the use of DNS database has rapidly spread in the turbulence research community. DNSs are three-dimensional, time-dependent numerical solutions of the governing Navier–Stokes and scalar transport equations that compute the evolution of flow and scalar fields without using any turbulence models. Hence, a DNS must be executed on a three-dimensional grid system which is fine enough to resolve all significant scales arising in turbulent transport processes. Despite this demanding nature, DNS has proved to be a valuable tool for the fundamental research of turbulent transport phenomena (Reynolds, 1990; Kasagi and Shikazono, 1995).

In this paper, the numerical treatment for DNS is first reviewed and then the recent progress in the applications of DNS is illustrated by introducing two typical examples. In the DNS of a turbulent flow in a rotating plane channel, the buoyant and Coriolis forces are found to affect together the momentum and heat transfer mechanisms in a complex manner. Trial computations for possible active turbulence control are also presented. The most efficient spatio-temporal distribution of the control input is determined by adopting a new control theory. The author's views on future development are given, when appropriate. Thus, this paper is not intended to be a comprehensive review on DNSs of turbulent transport phenomena; for general reviews readers are referred to, e.g., Reynolds (1990), Kasagi and Shikazono (1995), Rogallo and Moin (1984), Schumann and Friedrich (1987), Moin and Spalart (1989).

2. Numerical methods of direct numerical simulation

Because a turbulent flow contains a broad range of dynamically significant scales, its DNS must meet the following two requirements: (i) the computational domain should be large enough to contain the largest eddies, and (ii) the grid spacing should be fine enough to resolve the smallest eddies. Based on a crude estimate, the ratio of the largest to smallest length scales in a turbulent flow is proportional to the 3/4 power of the flow Reynolds number Re in each direction, so that the to-

[1] E-mail: kasagi@thtlab.t.u-tokyo.ac.jp.

0142-727X/98/$19.00
PII: S0142-727X(97)10017-0

tal number of grid points N required in a DNS is proportional to $Re^{9/4}$. The time increment in advancing the numerical integration should be as small as the smallest eddy's turnover time (and a Courant number should also be sufficiently small), whilst the total length of integration should be sufficiently larger than the largest eddy's turnover time in order to obtain converged turbulence statistics. The ratio of these largest to smallest time scales is roughly proportional to $Re^{1/2}$. Thus, as the Reynolds number increases, the numbers of grid points and time steps should increase rapidly; e.g., the number of grids required even for $Re = 10000$ reaches $N = 10^9$, and such a computation is hardly possible with most of the current supercomputers. However, if the bulk of the actual dissipation occurs at scales considerably larger than the Kolmogorov microscales, DNSs may be possible at Reynolds numbers on the order of $10^3 \sim 10^4$ (Rogallo and Moin, 1984); actually this was the case for the DNS of turbulent channel flow of Kim et al. (1987).

The above requirement of DNS is even more serious, once additional scales, which are out of the range of turbulence scales, are introduced or imposed. For example, scalar microscales should also be captured when turbulent scalar transport is to be simulated (Kim and Moin, 1989; Kasagi and Shikazono, 1995), but it becomes very difficult when a Prandtl or Schmidt number is large. The essentially same problem arises in flows with chemical reactions (combustion). In a flow along a wall with riblets (streamwise micro-groves), a large computational volume is hard to retain, because more grid points are required in order to reproduce the riblet shape with a sharp ridge (Choi et al., 1993a). In the simulations of multiphase flows, characteristic scales of interface deformation (or waves) and of distributed particles do not always stay within the range of turbulence scales, yet have remarkable interactions with turbulence. In flows under arbitrarily imposed unsteadiness, associated time scales must also be captured. These facts will be a major difficulty in DNSs of complex turbulent flows to be challenged in the future.

Despite the above severe demands inherent in DNS, continuous efforts have been directed to improvement of the numerical treatments for spatio-temporal discretization. Spatial discretization schemes for DNS are categorized into spectral (Canuto et al., 1987), spectral element (Patera, 1984) and finite difference (Peyret and Taylor, 1983) methods. Because of its exponential convergence, the spectral method should be most suitable to DNS, in which high spatial resolution is required. It needs, however, linearization of governing equations with explicit or semi-implicit time advancement schemes. The channel flow simulation of Kim et al. (1987) is based on a spectral method, which employs Fourier series in the two periodic directions and Chebyshev polynomial expansion in the wall-normal direction. The spectral method can be extended to geometrically complex flows by using mapping (coordinate transformations) or patching (Orszag, 1980). The former is used in the adaptive spectral method, which has been successfully adopted in the DNSs of turbulent boundary layers (Spalart and Leonard, 1987), square duct flows (Madabhushi et al., 1993), turbulent flows over three- dimensional bumps (Carlson and Lumley, 1996) and gas–liquid interfacial turbulence (Lombardi et al., 1996).

The spectral element technique can be interpreted as a high-order finite element method or a patching mode of the spectral method (Peyret and Taylor, 1983). It has both flexibility of finite element method and exponential convergence of spectral method. A DNS of turbulent flow over riblets has been performed by Chu and Karniadakis (1993) using this technique.

Applicability of a high-order finite difference scheme (Rai and Moin, 1991, 1993) and a compact finite difference scheme (Adam, 1977; Hirsh, 1977; Lele, 1992) to DNS has been illustrated. The former was employed in the DNS of turbulent boundary layers by Rai and Moin (1993). In addition, the second-order finite difference scheme (with a fractional step method) has shown great adaptability for various kinds of flows such as square duct turbulence (Gavrilakis, 1992), turbulent flow over riblets (Choi et al., 1993a), three-dimensional flow in a curved square duct (Zang et al., 1994) and turbulent flow along an oscillatorily deformed wall (Mito and Kasagi, 1997).

Temporal discretization schemes adopted so far are an explicit scheme, a semi-implicit scheme (a combination of implicit and explicit schemes), and a fractional step method (Chorin, 1969; Temam, 1984). The semi-implicit scheme, with Adams–Bashforth method used for the nonlinear terms and Crank–Nicolson method for the linear terms, was adopted in the channel flow DNS by Kim et al. (1987), whilst the third-order Runge–Kutta method (Spalart et al., 1991) has also become popular.

A fractional step method developed by Chorin (1969) and Temam (1984) is employed in many DNSs. By choosing this scheme, solutions for velocity and pressure fields can be separated, and this leads to appreciable reduction in computational load. Kim and Moin (1985) uses a semi-implicit type fractional step method, with Adams–Bashforth method being applied to the nonlinear terms and Crank–Nicolson method to the linear terms. This method has been improved to a higher-order version by Rai and Moin (1991) and Le and Moin (1991), i.e., with a low-storage third-order Runge–Kutta method (Spalart et al., 1991) and Crank–Nicolson method. A four-step time advancement scheme of Choi and Moin (1994) is a second-order Crank–Nicolson type fractional step method, which employs a delta-form to the pressure gradient terms. This scheme is more accurate and stable, although the computation may be heavier because of nonlinear couplings (Mito and Kasagi, 1997).

It is noted that many of the recent DNS applications are also found in the research on multiphase turbulent flows. Gas–liquid interfaces, bubbles and particles are taken into account by sophisticated numerical techniques, e.g., so-called level set (Sussman et al., 1994), CIP (Yabe and Aoki, 1991) and force (Fogelson and Peskin, 1988) methods. In particle-laden flows, there take place interactions between fluid and particles, which should be numerically handled with (McLaughlin, 1994). In some cases called one-way coupling, only the force experienced by particles is taken into account (Pedinotti et al., 1992), but care must be taken of the degree of approximation in the equation of particle motion and also of the interpolation technique for the velocity field calculated by DNS. Much fewer computations for two-way coupling have been reported (Elghobashi and Truesdell, 1993).

3. Applications of direct numerical simulation

3.1. Significance and novelty of DNS

A DNS can be regarded as a numerical experiment which replaces a laboratory experiment. Although the Reynolds number remains small to moderate, there are many attractive and advantageous features in DNS, and among them the following points are to be worth mentioning (Kasagi and Shikazono, 1995):

(1) DNS should be superior to experimental measurement in permitting one to probe all the instantaneous flow variables such as velocities, pressures, vorticities and temperatures in three-dimensional space. Hence, turbulent structures and transport mechanisms can be extensively analyzed through various theoretical approaches and visualization techniques (Robinson, 1991; Kasagi et al., 1995).

(2) Even experimental measurement techniques can be tested and evaluated in numerically simulated turbulent flow and thermal fields (Moin and Spalart, 1989; Suzuki and Kasagi, 1992).

(3) DNSs can provide precise and detailed turbulence statistics including pressure and any spatial derivatives, which are undoubtedly of great help for evaluating and developing turbulence models. The statistics and their budgets in various types of flows are available in tabulated forms at ftp sites (e.g., http://www.thtlab.t.u-tokyo.ac.jp and http://fluindigo.-mech.surrey.ac.uk).

(4) Important parameters characterizing flow and scalar fields, e.g., Reynolds, Prandtl, Richardson, Rossby, and Hartmann numbers, can be systematically varied in DNSs. For example, heat transfer over a Prandtl number range (Kim and Moin, 1989; Kasagi et al., 1992; Kasagi and Ohtsubo, 1993) should preferably be studied in DNS databases, which are usually more reliable and consistent than experimental data. The effects of buoyancy (Iida and Kasagi, 1996; Kasagi and Nishimura, 1997), wall injection/suction (Sumitani and Kasagi, 1995) and a MHD force (Noguchi and Kasagi, 1994) can be examined.

(5) Lastly, DNS can offer a chance to study even a virtual flow field which would not occur in reality. This is particularly meaningful in studying some particular dynamical aspect of a turbulence phenomenon (Jimenez and Moin, 1991) or evaluating possible turbulence control methodologies (Jung et al., 1992; Choi et al., 1994; Satake and Kasagi, 1996).

All of these aspects illustrate novelty and superiority of DNSs, of which exploitation must be quite helpful and advantageous in current and future turbulence research. The following sections describe two of the recent applications, which would demonstrate such distinctive merits of DNS.

3.2. DNS of complex turbulent flow and heat transfer

The recent trend of DNSs seems to be characterized by an increasing degree of complexity and diversity of simulated turbulent flow phenomena. The applications have been considerably extended, e.g., homogeneous to inhomogeneous, spatio-temporally stationary to developing, incompressible to compressible, and single-phase to multiphase flows. Those with moving boundaries and with chemical reactions have also been tackled. Among them, a problem arises when two or more dynamical effects appear together in a complex manner, which cannot be predicted straightforward from the observation under each of those effects alone. The friction and heat transfer coefficients may not change in the way as might be expected by the conventional analogy rule. One of the dynamically complex turbulent flows with heat transfer was recently studied by Nishimura and Kasagi (1996). It was the combined forced and natural turbulent convection flow in a rotating channel, which is of obvious engineering interest, since its applications are often found in rotating machinery such as coolant passages in a turbine blade (Han and Zhang, 1992). The experimental measurement, however, should be extremely difficult. Thus, the coupled effect of system rotation and centrifugal buoyancy on the fully developed turbulent channel flow was investigated through a series of DNSs.

A constant pressure gradient drives the mean flow between the two parallel walls kept at different temperatures, while the whole channel is rotated at a prescribed angular velocity around its spanwise axis as shown in Fig. 1. The Coriolis force may, for instance, enhance the turbulence along the pressure side of a coolant passage in a turbine blade and simultaneously reduce the turbulent activity along the suction side (P- and S-sides, respectively, hereafter) as discussed by Johnston et al. (1972). Moreover, depending upon whether the buoyancy

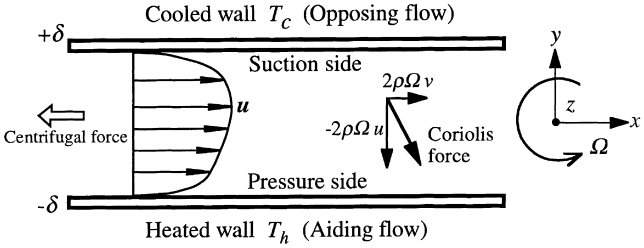

Fig. 1. Rotating channel flow and coordinate system.

force is acting to aid or oppose the forced flow (A- and O-flows, hereafter), the turbulence is drastically decreased or increased (Kasagi and Nishimura, 1997). Thus, the interaction takes place between the dynamical and thermal characteristics, which are known to appear on the pressure and suction sides of the rotating channel due to the Coriolis force, and those in the aiding and opposing flows due to the streamwise buoyant force.

The governing equation for the velocity vector of an incompressible flow in a channel rotating around its spanwise axis can be given in the following dimensionless form with the Boussinesq approximation:

$$\frac{\mathrm{D}\mathbf{u}}{\mathrm{D}t} = -\mathbf{p}\frac{1}{\mathrm{Re}_\tau^*}^2\mathbf{u} - \mathrm{Ro}_\tau^*\mathbf{e}_3 \times \mathbf{u} - \frac{1}{8}\frac{\mathrm{Gr}}{\mathrm{Re}_\tau^{*2}}\left(\theta + \frac{T_c - T_0}{\Delta T}\right)\mathbf{e}_1, \qquad (1)$$

where $\mathbf{e}_1 = (1,0,0)$, $\mathbf{e}_3 = (0,0,1)$, and the variables and parameters are nondimensionalized by the channel half-width δ, the friction velocity u_τ^*, and the temperature difference between the two walls ΔT. Then, the three independent dimensionless parameters specifying the flow conditions are the Reynolds number, Re_τ^* $(= u_\tau^*\delta/\nu)$, the rotation number, $\mathrm{Ro}_\tau^*(= 2\Omega\delta/u_\tau^*)$, and the Grashof number, $\mathrm{Gr}(= \beta\Omega^2 R\Delta T(2\delta)^3/\nu^2)$. Note that the radius of rotation R in Gr is assumed to be constant, because it is intended to simulate coolant passages in a turbine blade, of which height should be very small compared to the turbine rotor disc radius. The Reynolds number Re_τ^* based on the wall friction velocity u_τ^* and the channel half-width δ is 150. Note that u_τ^* is calculated from the wall shear stress averaged on the two walls. The Prandtl number Pr is assumed to be 0.71, while the rotation number is changed as $\mathrm{Ro}_\tau^* = 0$ and ± 1.5.

The governing momentum, energy and continuity equations were solved simultaneously by using the pseudo-spectral method with Fourier and Chebychev expansions in the homogeneous and wall-normal directions, respectively. The flow and thermal fields were assumed to be fully developed, so that the periodic boundary conditions were imposed at the periods of $5\pi\delta$ and $2\pi\delta$ in the x- and z-directions, respectively. The details of the numerical method are found in Kasagi et al. (1992) and Kasagi and Nishimura (1997).

In this DNS, two rotation numbers are chosen, so that four independent combinations of the two kinds of dynamical influences are investigated as indicated in Table 1 (denoted as P-A, S-O, S-A, and P-O). It is noted that, in the DNS of combined convection in a vertical channel (Kasagi and Nishimura, 1997), with the opposing buoyancy the mean flow is decelerated while the turbulence is activated, and the opposite change is observed with the aiding one.

The mean velocity distributions across the channel width are shown in Fig. 2(a), where the vertical axis is nondimensionalized by u_τ^*. The two results on the P-side show a quite similar change, i.e., a fuller profile and a steeper velocity gradient near the wall, apparently with little buoyancy effect. The flows on the S-side are seen oppositely affected with the near-wall gradients reduced, particularly on the S-O side.

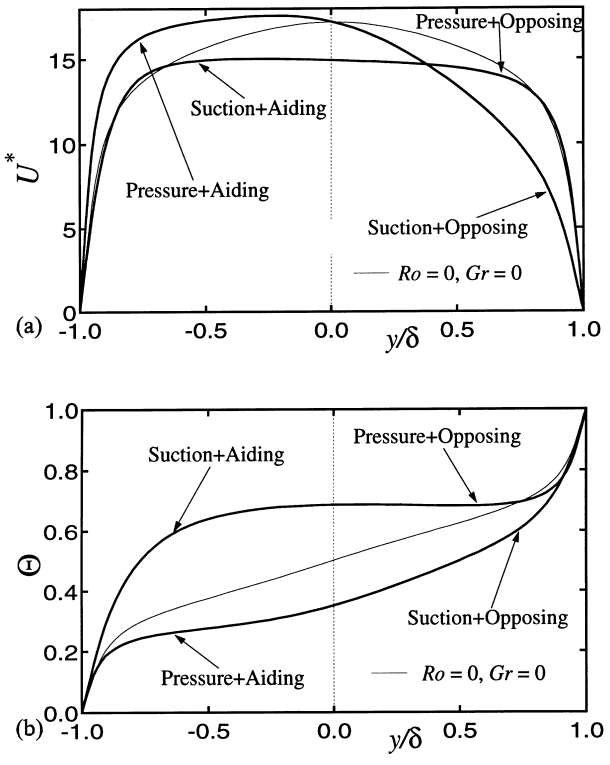

Fig. 2. Mean flow distributions: (a) velocity; (b) temperature.

These changes in the mean flow field result in the friction coefficient C_f summarized in Table 1; it is largest in the P-A flow, where both rotation and buoyancy tend to increase the mean velocity, and hence velocity gradient, near the wall. On the other hand, it is smallest in the S-O flow.

In Fig. 2(b), the dimensionless mean temperature profile shows little change near the wall, although its level in the central part of the channel is drastically changed by the relative magnitudes of the heat transfer resistances on the two opposite wall regions. In Table 1, the heat transfer coefficient shows characteristics different from C_f as in Kasagi and Nishimura (1997); the P-O and S-A flows give the highest and lowest heat transfer rates, respectively. This is because, in a fully developed channel, unlike C_f the heat transfer is only sensitive to turbulent transport, but not to the mean flow field. As a result, the analogy between momentum and heat transfer does not hold in these cases. On the P-O side, the temperature gradient becomes slightly negative, indicating that a counter-gradient heat flux takes place there. Also note that the overall heat transfer rate (see, $\mathrm{Nu}^* = 2q_w\delta/(\lambda\Delta T)$) is about 20% different depending upon the direction of rotation.

The root-mean-square fluctuations are represented in Fig. 3. Unlike the mean field parameters discussed above, these statistics reflect very complex coupled effects of rotation and buoyancy. It is natural to expect the largest fluctuations in the P-O flow because each of the two effects would enhance turbulence, but it is the case only in the v and w velocity components. The u component is largest in the P-A flow. In the S-A flow, turbulence would be most attenuated, but only the v component is much decreased, and this is confirmed to result in a reduced production rate of the Reynolds shear stress. In the S-O flow, u_{rms} is diminished remarkably, whereas v_{rms} and w_{rms} are not much modified, so that the stress anisotropy should be very much reduced.

The temperature fluctuation in most flows is known to be highly correlated with u, but behaves much differently in Fig. 3(d). In the S-A flow, although u_{rms} is considerably large, θ_{rms} is even more large. In this case the heat flux is separately found to remain moderate and this low correlation between the v and θ fluctuations means that the temperature fluctuation is not caused by active turbulent mixing, but large-scale motions discussed later. On the two P-sides, the buoyancy effect changes θ_{rms} as one expects, but the decrease on the P-A side is in marked contrast to u_{rms}. Likewise, θ_{rms} and u_{rms} on the S-O side exhibit opposite changes.

As in the drastic change in the statistical quantities, the turbulent structures are also influenced by the combined effect of rotation and buoyancy as shown in Fig. 4, where the rotation number is increased to $\mathrm{Ro}_\tau^* = 2.5$. The top and bottom figures visualize the so-called low-speed streaks and the streamwise vortical structures (indicated as local low-pressure regions) near the two walls in the cases of S-A and P-O sides, and the middle shows the vector diagram with the gradation contour of streamwise velocity fluctuations. It is obvious that enhanced turbulence with smaller scale motions dominates the wall region on the P-O side, while the turbulence structures fade away and even disappear locally on the S-A side. In addition, roller-like secondary flow patterns can be observed in the central part of the channel, and they should be responsible for the extraordinary large temperature fluctuation on the S-A side and the counter-gradient heat flux on the P-O side.

3.3. DNS of active turbulence control

Turbulence control has been one of the central issues in modern scientific, engineering and environmental research efforts. Its potential benefits can be easily recognized if one thinks about the significance of the artificial manipulation of turbulent drag, noise, heat transfer as well as chemical reaction, to name a few. Among various efforts, many intensive investigations have been undertaken focusing on possible drag reducing techniques over the decades. Although there is considerable empirical knowledge on passive control methods such as polymers, riblets and LEBU, efforts are now directed

Table 1
Friction and heat transfer coefficients [a] in a rotation channel with buoyancy

	Standard	Pressure and aiding	Suction and opposing	Suction and aiding	Pressure and opposing
Gr	–		9.6×10^5		
Ro_τ^*	–	−1.5		+1.5	
Re_b	4351	4266		4046	
C_f	9.499×10^{-3}	1.281×10^{-2}	4.832×10^{-3}	1.066×10^{-2}	1.173×10^{-2}
Nu	14.51	17.54	12.78	8.485	29.30
Nu^*	5.50	5.80		6.90	

[a] C_f and Nu are defined based on the bulk-averaged velocity and temperature, respectively, which are calculated over the subregion from the wall to the maximum velocity location.

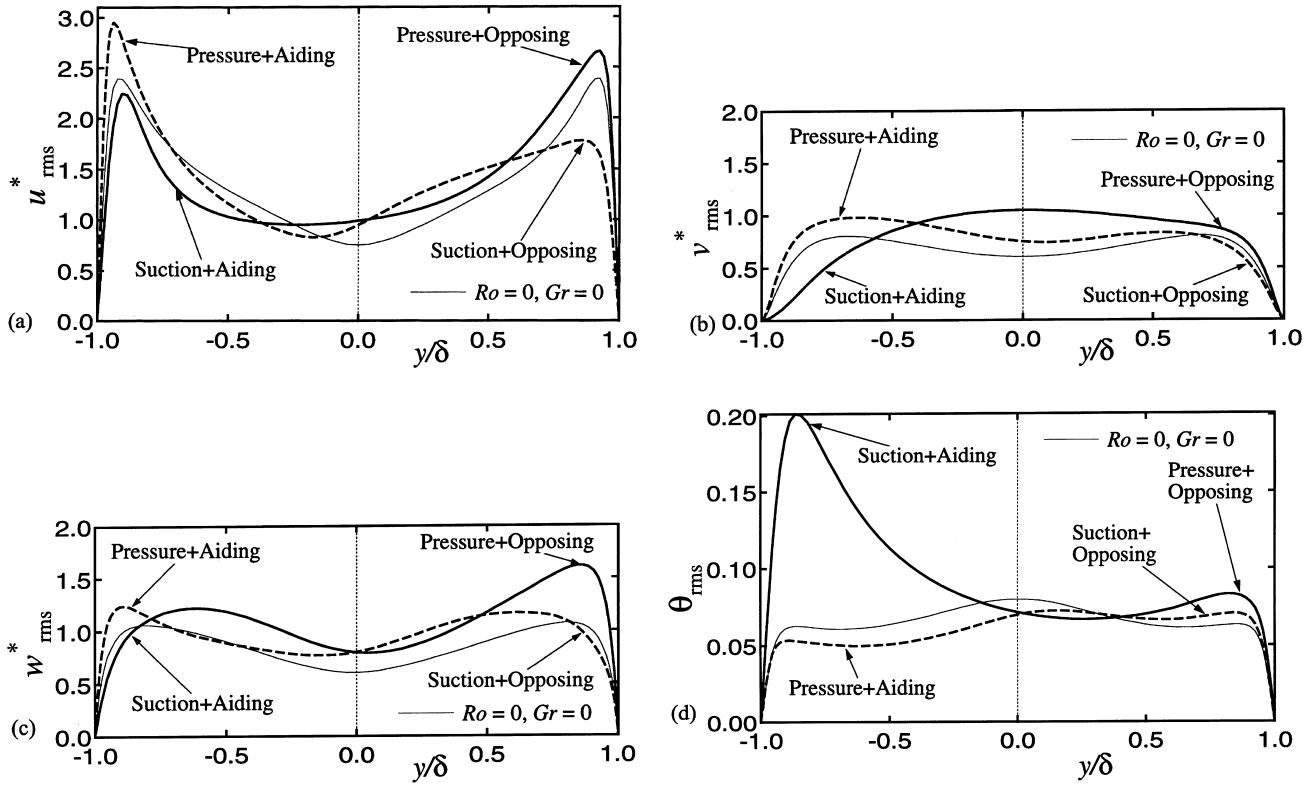

Fig. 3. Root-mean-square fluctuations: (a) streamwise; (b) wall-normal; (c) spanwise velocities and (d) temperature.

toward to interactive ones, particularly those exploiting emerging micromachining technology, called microelectromechanical systems (MEMS) (Moin and Bewley, 1994; Ho and Tai, 1996; Jacobson and Reynolds, 1993). The turbulent structures in real flows are very small in size, typically several hundred microns in width and a few mm in length in wall turbulence. Their lifetime is also very short. In the past, direct manipulation of these structures was very difficult, but is now expected to become possible with miniature sensors and actuators of micron size fabricated by MEMS. This new technology offers a batch production process, through which micromechanical parts are produced in large quantities. A MEMS controller unit, with its integrated mechanical parts and IC, will be able to sense the physical world, process the information, and then manipulate the physical phenomena through actuators. From this viewpoint, studies of active turbulence control now begin to use DNSs extensively for analyzing the effectiveness of proposed control algorithms (Choi et al., 1993b; Moin and Bewley, 1995; Satake and Kasagi, 1997; Lee et al., 1997) to lead the future development of MEMS controllers and systems.

There are some interesting attempts to control wall turbulence through the alternation of the spanwise fluid motion near the wall (Jung et al., 1992; Satake and Kasagi, 1996). In the simulation of Satake and Kasagi (1996), a turbulence control method for drag reduction is tested with a thin layer adjacent to the wall, where a body force acts to impede the spanwise velocity, as shown in Fig. 5. The virtual decelerating force, whose magnitude is proportional to the spanwise velocity, is introduced into the momentum equation as

$$\frac{D\mathbf{u}}{Dt} = -\mathbf{p} + \frac{1}{Re_\tau}{}^2\,\mathbf{u} - \alpha(\mathbf{u}\cdot\mathbf{e}_3)\mathbf{e}_3, \tag{2}$$

where the variables are nondimensionalized by the friction velocity and the channel half-width. The strength of the last term on the RHS of Eq. (2) is given by a dimensionless constant, $\alpha(>0)$. Nonzero values of α are assumed in a prescribed layer parallel to the wall. In a series of simulations, α is gradually increased up to 4, whereas in another series the damping layer of thickness $\Delta y^+ = 10$ is shifted away from the wall.

The Reynolds number, which is based on the wall friction velocity u_τ and channel half-width δ, is kept at 150 in all test cases. The computational domain is relatively small and similar to the "minimal flow unit" used in Jimenez and Moin (1991). Thus, the streamwise and spanwise computational periods are relatively small, i.e., 589 and 176 wall units, respectively. The number of grid points is $48 \times 97 \times 36$ in the x-, y- and z-directions, respectively.

The dependence of the skin friction coefficient C_f on the bulk-mean Reynolds number Re_b is shown in Fig. 6. Although the skin friction coefficient C_{f0} for the ordinary case ($\alpha = 0$) has a slight deviation from the empirical formula of Dean (1978), it is clearly seen that the friction coefficient is decreased appreciably in all cases with $\alpha \neq 0$. Note that the bulk Reynolds number is increased in drag-reducing cases, because the streamwise mean pressure gradient is kept constant in the simulations.

The effect of the damping layer location is shown in Fig. 7. The largest reduction to about 85% in the ratio of C_f/C_{f0} is obtained when the damping is applied over the region of $0 < y^+ < 10$; this location is found more effective than the regions away from the wall. The Nusselt number is similarly decreased in these controlled channel flows. It is of interest that the turbulent flow field is most affected by the local w-damping when it is imposed beneath or above, but not *in* the buffer layer where the turbulent production rate is maximum.

The efficiency of the process under study is evaluated by referring to Choi et al. (1994), i.e., by estimating the ratio of the pumping power saved to the damping dissipation rate (or the work required for control):

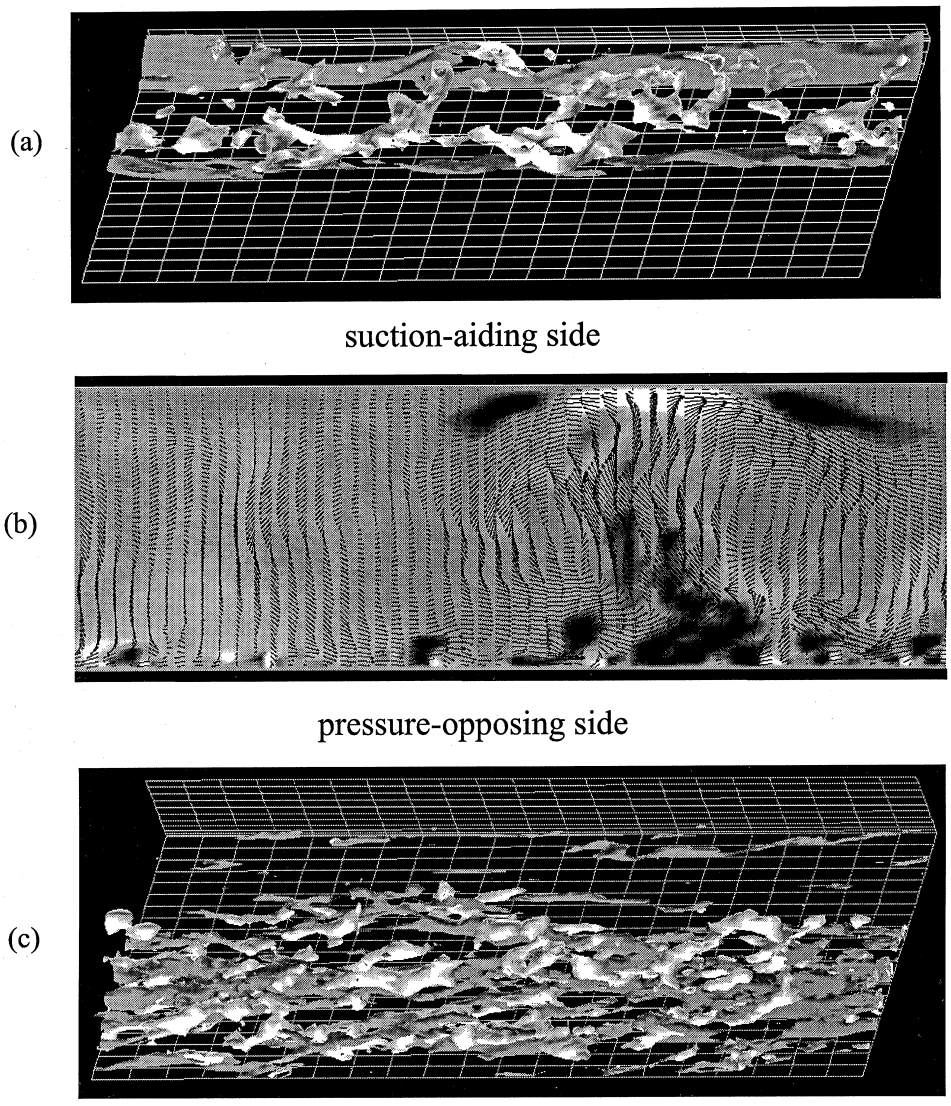

Fig. 4. Low-pressure and low-speed regions visualized on the suction-aiding and pressure-opposing sides (a,c), and velocity vector diagram in the cross stream plane (b) ($Ro_\tau^* = 2.5, Gr = 9.6 \times 10^5$): gray, $u/(u_{rms})_{max} = 1$, white, $p/(p_{rms})_{max} = 1.3$.

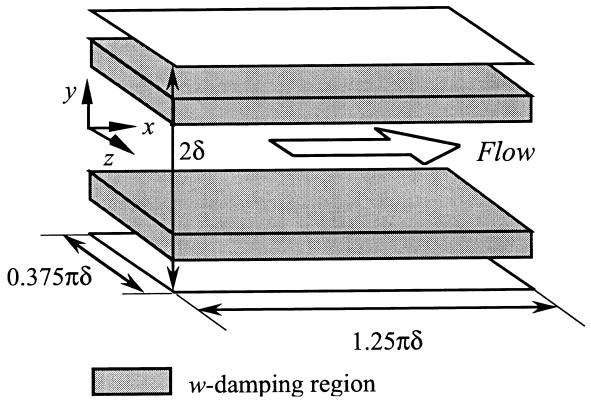

Fig. 5. Computational volume and coordinates.

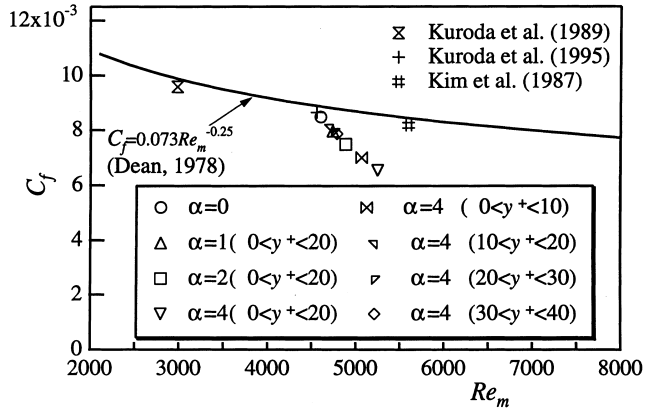

Fig. 6. Skin-friction coefficient.

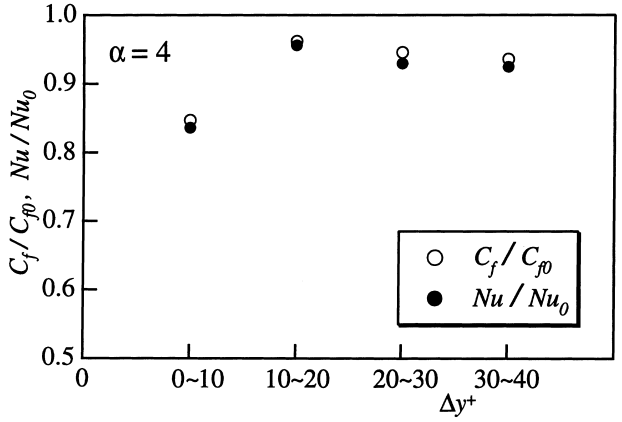

Fig. 7. Effect of the location of damping layer on friction coefficient (open symbols) and Nusselt number (closed symbols).

$$\eta = \left[\left(-\mathrm{d}\overline{p}^{+}/\mathrm{d}x^{+}\,|_{\mathrm{u}} + \mathrm{d}\overline{p}^{+}/\mathrm{d}x^{+}\,|_{\mathrm{d}}\right)\langle U\rangle^{+}\right]/\frac{1}{V}\int_{V}\alpha\overline{w^{+}w^{+}}\,\mathrm{d}V/\mathrm{Re}_{\tau}, \tag{3}$$

where the first and second terms in the numerator are the mean pressure gradients in the ordinary and w-damped channels, respectively, and V denotes the computational volume. The dependence of the efficiency on the damping layer location when $\alpha = 4$ is represented in Fig. 8. The above efficiency at $0 < y^{+} < 10$ becomes the largest and about 80, indicating that the damping dissipation should be negligible.

Although modern knowledge on the structure of turbulent flow is successfully exploited in choosing the effective mode of manipulation and attenuation in the above DNS, the underlying mechanism might not have been fully explored. Likewise, in many cases an attempt at optimizing the turbulence control is likely to be based on empiricism or intuition. Then, a question arises whether the spatio-temporal distribution of control input can be optimized in the sense that the maximum control performance is achieved with the least control input energy.

Recently, Choi et al. (1993b) devised a suboptimal feedback control algorithm for the Navier–Stokes equations and applied it to the stochastic Burgers equation. As a result, the proposed control method produced significant reduction in the cost functions defined. Their suboptimal control algorithm can be implemented in real applications in contrast to the optimal control theory (Abergel and Temam, 1990). The latter provides more ideally optimized control distributions, but cannot be applied in reality because of its extremely heavy computational load. Choi (1995) applied the suboptimal control algorithm to a turbulent channel flow and a vortex shedding behind a circular cylinder. The control method used in his study is an extended version of the algorithm developed in Choi et al. (1993b) and Moin and Bewley (1995).

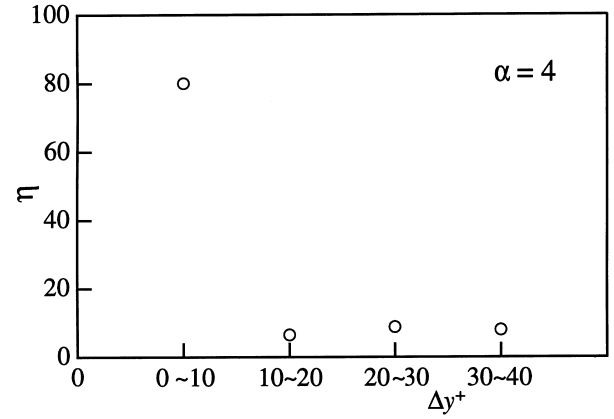

Fig. 8. Ratio of pumping power saved to damping dissipation.

Satake and Kasagi (1997) extended the work mentioned above and tried to design the spatial distribution of body force with the suboptimal control theory. Trial cost functional to be minimized is defined by referring to the kinematic states of the quasi-coherent vortical structures. Then, the suboptimal control scheme is implemented numerically in the DNS of turbulent channel flow. The governing equations to describe the flow are again given by Eq. (2), but the strength of the virtual body force α is now a function of time and location in the region of $0 < y^{+} < 10$, and its distribution is to be determined by the suboptimal control algorithm.

The two cost functionals are defined as:

$$J_1(\alpha) = \frac{\ell}{2}\int_{V}\alpha^2 C(x_2)\,\mathrm{d}V + \frac{m}{2}\int_{V}\left(\frac{\partial u_3}{\partial x_2}\right)^2 C(x_2)\,\mathrm{d}V, \tag{4a}$$

$$J_2(\alpha) = \frac{\ell}{2}\int_{V}\alpha^2 C(x_2)\,\mathrm{d}V + \frac{m}{2}\int_{V}\left(\frac{\partial u_3}{\partial x_3}\right)^2 C(x_2)\,\mathrm{d}V, \tag{4b}$$

where ℓ and m are weighting parameters. These equations are multiplied by $C(x_2)$, which is 1 when $0 < y^{+} < 10$ and zero otherwise, to limit the damping effect to the wall-attached region. The first terms in Eqs. (4a) and (4b) are a measure of the magnitude of the control input, whereas the second terms represent the quantities to be reduced. It is noted that the latter in Eqs. (4a) and (4b) correspond to the major components of the rotation and strain rates, respectively, that are associated with the quasi-coherent streamwise vortex near the wall (Iida and Kasagi, 1993).

The relative magnitude of ℓ against m should be modified according to the cost and the degree of importance of the control; ℓ can be very small when the control is cheap and easy to implement. In Satake and Kasagi (1997), four different cases are tested with the two cost functionals defined by Eqs. (4a) and (4b) with two different weighting parameters as listed in Table 2. These values of ℓ and m are quite arbitrarily chosen. Another parameter ρ in Table 2 is a descent coefficient, which is used in the gradient algorithm to renew the distribution of the control input at every time step.

The time histories of the mean pressure gradient over the computational period with and without control are shown in Fig. 9. The suboptimal results are also compared with those obtained in the cases with constant α, which has been changed as $\alpha = 4$, 10 and 100. The effect of the control appears distinctively in all controlled flows, once the control is started. Note that the smallest possible value of about 0.3 in Fig. 9 is obtained when the flow becomes completely laminar. Hence, about half of the possible drag reduction is achieved in Cases 3 and 4. Almost equivalent control performance can be obtained with $\alpha = 100$, but the energy consumption is larger if compared with the suboptimal control.

The results presented here are brought about by introducing the suboptimal control theory, whereas different types of active feedback control algorithms based upon adaptive schemes and dynamical systems theory are also being intensively studied (Moin and Bewley, 1994). In particular, a nonlinear adaptive algorithm, called neural networks, has a wide range of applicability (Jacobson and Reynolds, 1993; Lee et al., 1997), since it does not require precise mathematical description of the system nor empirical knowledge on physical mechanisms. These new proposals for smart turbulence con-

Table 2
Parameters for suboptimal control

Case	Cost functional	ℓ	m	ρ
1	$J_1(\alpha)$	1	1000	0.01
2	$J_2(\alpha)$	1	1000	0.01
3	$J_1(\alpha)$	0	1	10
4	$J_2(\alpha)$	0	1	10

trol should also be tested and evaluated through the further use of DNSs.

4. Concluding remarks

With high performance supercomputers, reliable numerical methods and efficient post-processing environment, direct numerical simulation offers valuable numerical experiments for turbulence research. A variety of exploitation of DNS will be possible. In particular, with all instantaneous flow variables, one can extensively study the dynamics and transport mechanisms of turbulence through three-dimensional visualization of physical quantities of interest. It is also possible to establish detailed database of various turbulence statistics in turbulent transport phenomena, while systematically changing important flow and scalar field parameters.

The present paper has concentrated on new findings recently obtained by the author's group. In the first example, the coupled effect of buoyant and Coriolis forces on turbulent transport is investigated in a rotating channel flow. The two dynamical effects are found to appear in a complex nonlinear manner, which cannot be predicted from the behavior under each of the two effects. The friction and heat transfer coefficients do not change in the way as expected by the conventional analogy theory. The latter is highest with the turbulent transport most activated in the opposing flow on the pressure (P-O) side, while it is lowest in the aiding flow on the suction (S-A) side. In the central region between the P-O and S-A sides, there are observed the large-scale roller-like streamwise vortices, which should cause markedly large temperature fluctuations on the S-A side and the counter-gradient heat flux on the P-O side.

In the second example, a series of DNSs have been carried out of the channel flow under an active turbulence control, which imposes a thin w-damping layer in the vicinity of the wall. It is found that the w-damping brings about notable reduction in the turbulent friction drag. The extra work due to the w-damping remains negligible as long as the damping layer exists close to the wall. In addition, it is illustrated that this control method can be more efficient if the spatio-temporal distribution of the damping force is optimally designed by a control theory.

There are yet many complex but important problems of turbulent transport such as multiphase flows and those with chemical reactions, of which DNSs should be challenged. In addition, DNS will be even more useful in evaluating future turbulence control methodologies based on new algorithms such as optimum control theory and neural networks. These simulations have been triggered by the rapid development of MEMS technology, but hopefully future DNSs will lead further development of MEMS-based controller units integrating microsensors, microactuators and CPUs. Thus, there is no doubt that DNS will serve continuously as a powerful tool for fundamental turbulence research in the coming century.

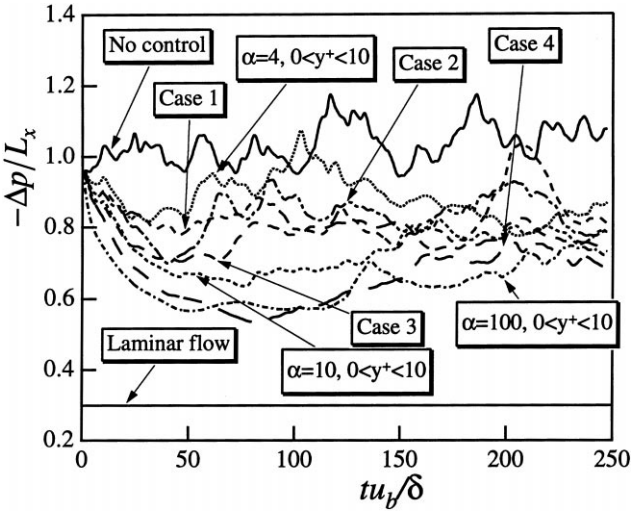

Fig. 9. Mean pressure gradient in controlled channel flow.

Acknowledgements

The author thanks Drs. S. Satake and Y. Mito, and Mr. M. Nishimura for their aids in preparing the present manuscript. This work was supported by the Ministry of Education, Science and Culture through the Grant-in-Aid for Scientific Research on Priority Areas (No. 05240103).

References

Abergel, F., Temam, R., 1990. On some control problems in fluid mechanics. Theor. Comput. Fluid Dyn. 1, 303–325.

Adam, Y., 1977. High accurate compact implicit methods and boundary conditions. J. Comput. Phys. 24, 10–22.

Canuto, C., Hussaini, M.Y., Quarteroni, A., Zang, T.A. 1987. Spectral Method in Fluid Dynamics. Springer, Berlin.

Carlson, H.A., Lumley, J.L., 1996. Active control in the turbulent wall layer of a minimal flow unit. J. Fluid Mech. 329, 341–371.

Choi, H., 1995. Suboptimal control of turbulent flow using control theory. In: Proceedings of the International Symposium on Math. Model. Turbulent Flows, Tokyo, pp. 131–138.

Choi, H., Moin, P., 1994. Effects of the computational time step on numerical schemes of turbulent flow. J. Comput. Phys. 113, 1–4.

Choi, H., Moin, P., Kim, J., 1993a. Direct numerical simulation of turbulent flow over riblets. J. Fluid Mech. 255, 503–539.

Choi, H., Moin, P., Kim, J., 1994. Active turbulence control for drag reduction in wall-bounded flows. J. Fluid Mech. 262, 75–110.

Choi, H., Temam, P., Moin, P., Kim, J., 1993b. Feedback control for unsteady flow and its application to the stochastic Burgers equation. J. Fluid Mech. 253, 509–543.

Chorin, A.J., 1969. On the convergence of discrete approximations to the Navier–Stokes equations. Math. Comput. 23, 341–353.

Chu, D.C., Karniadakis, G.E., 1993. A direct numerical simulation of laminar and turbulent flow over riblet-mounted surfaces. J. Fluid Mech. 250, 1–42.

Dean, R.B., 1978. Reynolds number dependence of skin friction and other bulk flow variables in two-dimensional rectangular duct flow. ASME J. Fluids Eng. 100, 215–223.

Elghobashi, S., Truesdell, G.C., 1993. On the two-way interaction between homogeneous turbulence and dispersed solid particles. 1: Turbulence modification. Phys. Fluids A 5, 1790–1801.

Fogelson, A.L., Peskin, C.S., 1988. A fast numerical method for solving the three-dimensional Stokes equations in the presence of suspended particles. J. Comput. Phys. 79, 50–69.

Gavrilakis, S., 1992. Numerical simulation of low-Reynolds-number turbulent flow through a straight square duct. J. Fluid Mech. 244, 101–129.

Han, J.-C., Zhang, Y.M., 1992. Effect of uneven wall temperature on local heat transfer in a rotating square channel with smooth walls and radial outward flow. ASME J. Heat Transfer 114, 850–858.

Hirsh, R.S., 1977. High order accurate difference solutions of fluid mechanics problems by a compact differencing technique. J. Comput. Phys. 19, 90–109.

Ho, C.-M., Tai, Y.-C., 1996. Review: MEMS and its applications for flow control. ASME J. Fluids Eng. 118, 437–447.

Iida, O., Kasagi, N., 1993. Redistribution of the Reynolds stresses and destruction of the turbulent heat flux in homogeneous decaying turbulence. In: Proceedings of the Ninth Turbulent Shear Flows, Kyoto, 3, pp. 24.4.1–24.4.6.

Iida, O., Kasagi, N., 1996. Direct numerical simulation of unstably stratified turbulent channel flow. ASME J. Heat Transfer 119, 53–61.

Jacobson, S.A., Reynolds, W.C., 1993. Active control of boundary layer wall shear stress using self-learning neural networks. AIAA Paper 93–3272.

Jimenez, J., Moin, P., 1991. The minimal flow unit in near-wall turbulence. J. Fluid Mech. 225, 213–240.

Johnston, J.P., Halleen, R.M., Lezius, D.K., 1972. Effects of spanwise rotation on the structure of two-dimensional fully developed turbulent channel flow. J. Fluid Mech. 25, 533–557.

Jung, W.J., Mangiavacchi, N., Akhavan, R., 1992. Suppression of turbulence in wall-bounded flows by high-frequency spanwise oscillations. Phys. Fluids A 4, 1605–1607.

Kasagi, N., Nishimura, M., 1997. Direct Numerical simulation of combined forced and natural turbulent convection in a vertical plane channel. Int. J. Heat and Fluid Flow 18, 88–99.

Kasagi, N., Ohtsubo, Y., 1993. Direct numerical simulation of low Prandtl number thermal fluid in a turbulent channel flow. In: Durst, F. et al. (Eds.), Turbulent Shear Flows, vol. 8. Springer, Berlin, pp. 97–119.

Kasagi, N., Shikazono, N., 1995. Contribution of direct numerical simulation to understanding and modeling turbulent transport. Proc. Roy. Soc. London. Ser. A 45, 257–292.

Kasagi, N., Sumitani, Y., Suzuki, Y., Iida, O., 1995. Kinematics of the quasi-coherent vortical structure in near-wall turbulence. Int. J. Heat and Fluid Flow 16, 2–10.

Kasagi, N., Tomita, Y., Kuroda, A., 1992. Direct numerical simulation of the passive scalar field in a turbulent channel flow. ASME J. Heat Transfer 114, 598–606.

Kim, J., Moin, P., 1985. Application of a fractional-step method to incompressible Navier–Stokes equations. J. Comput. Phys. 59, 308–323.

Kim, J., Moin, P., 1989. Transport of passive scalars in a turbulent channel flow. In: Andre, J.-C. et al. (Eds.), Turbulent Shear Flows, vol. 6. Springer, Berlin, pp. 85–96.

Kim, J., Moin, P., Moser, R.D., 1987. Turbulence statistics in fully developed channel flow at low Reynolds number. J. Fluid. Mech. 177, 133–166.

Le, H.L., Moin, P., 1991. An improvement of fractional step methods for the incompressible Navier–Stokes equations. J. Comput. Phys. 92, 369–379.

Lee, C., Kim, J., Babcock, D., Goodman, R., 1997. Application of neural network to turbulence control for drag reduction. Phys. Fluids 9, 1740–1747.

Lele, S.K., 1992. Compact finite difference schemes with spectral-like resolution. J. Comput. Phys. 103, 16–42.

Lombardi, P., Angelis, V.D., Banerjee, S., 1996. Direct numerical simulation of near-interface turbulence in coupled gas–liquid flow. Phys. Fluids 8, 1643–1665.

Madabhushi, R.K., Balachandar, S., Vanka, S.P., 1993. A divergence-free Chebyshev collocation procedure for incompressible flows with two non-periodic directions. J. Comput. Phys. 105, 199–206.

McLaughlin, J.B., 1994. Numerical computation of particle-turbulence interaction. Int. J. Multiphase Flow 20, s211–s232.

Mito, Y., Kasagi, N., 1997. Turbulence modification with streamwise-uniform sinusoidal wall-oscillation. In: Proceedings of the 11th Symposium Turbulent Shear Flows, vol. 1, Grenoble, pp. 9.7–9.12.

Moin, P., Bewley, T., 1994. Feedback control of turbulence. Appl. Mech. Rev. 47, S3–S13.

Moin, P., Bewley, T., 1995. Application of control theory to turbulence. In: Proceedings of the Twelfth Australian Fluid Mechanics Conference, Sydney, pp. 10–15.

Moin, P., Spalart, P.R., 1989. Contributions of numerical simulation data bases to the physics, modelling, and measurement of turbulence. In: George, W.K., Arndt, R. (Eds.), Advances in Turbulence. Hemisphere, Washington, DC, pp. 11–38.

Moser, R.D., Moin, P., 1987. The effect of curvature in wall-bounded turbulent flows. J. Fluid Mech. 175, 479–510.

Nishimura, M., Kasagi, N., 1996. Direct numerical simulation of combined forced and natural turbulent convection in a rotating plane channel. In: Proceedings of the Third KSME-JSME Therm. Eng. Conf., vol. 3, Kyongju, 3, pp. 77–82.

Noguchi, H., Kasagi, N., 1994. Direct numerical simulation of liquid metal MHD turbulent channel flows (in Japanese). Prepr. JSME, No. 940-53, pp. 365–366.

Orszag, S.A., 1980. Spectral methods for problems in complex geometries. J. Comput. Phys. 37, 70–92.

Patera, A.T., 1984. A Spectral element method for fluid dynamics: Laminar flow in a channel expansion. J. Comput. Phys. 54, 468–488.

Pedinotti, S., Mariotti, G., Banerjee, S., 1992. Direct numerical simulation of particle behaviour in the wall region of turbulent flows in horizontal channels. Int. J. Multiphase Flow 18, 927–941.

Peyret, R., Taylor, T.D., 1983. Computational Methods for Fluid Flow. Springer, Berlin.

Rai, M.M., Moin, P., 1991. Direct simulations of turbulent flow using finite-difference schemes. J. Comput. Phys. 96, 15–53.

Rai, M.M., Moin, P., 1993. Direct numerical simulation of transition and turbulence in a spatially evolving boundary layer. J. Comput. Phys. 109, 169–192.

Reynolds, W.C., 1990. The potential and limitations of direct and large eddy simulations. In: Lumley, J.L. (Ed.), Whither Turbulence? – Turbulence at the Crossroads. Springer, Berlin, pp. 313–342.

Robinson, S.K., 1991. The kinematics of turbulent boundary layer structure. NASA TM-103859.

Rogallo, R.S., Moin, P., 1984. Numerical simulation of turbulent flows. Ann. Rev. Fluid Mech. 16, 99–137.

Schumann, U., Friedrich, R., 1987. On direct and large eddy simulation of turbulence. In: Comte-Bellot, G., Mathieu, J. (Eds.), Advances in Turbulence. Springer, Berlin, pp. 88–104.

Spalart, P.R., Leonard, A., 1987. Direct numerical simulation of equilibrium turbulent boundary layers. In: Durst, F. et al. (Eds.), Turbulent Shear Flows, vol. 5. Springer, Berlin, pp. 234–252.

Spalart, P.R., Moser, R.D., Rogers, M.M., 1991. Spectral methods for the Navier–Stokes equations with one infinite and two periodic directions. J. Comput. Phys. 96, 297–324.

Satake, S., Kasagi, N., 1996. Turbulence control with wall-adjacent thin layer damping spanwise velocity fluctuations. Int. J. Heat and Fluid Flow 17, 343–352.

Satake, S., Kasagi, N., 1997. Suboptimal turbulence control with the body force of selecteve velocity damping localized to the near-wall region. In: Proceedings of the Eleventh Symposium on Turbulent Shear Flows, vol. 1, Grenoble, pp. 1.43–1.48.

Sumitani, Y., Kasagi, N., 1995. Direct numerical simulation of turbulent transport with uniform wall injection and suction. AIAA J. 33, 1220–1228.

Sussman, M., Smereka, P., Osher, S., 1994. A level set approach for computing solution to incompressible two-phase flow. J. Comput. Phys. 114, 146–159.

Suzuki, Y., Kasagi, N., 1992. Evaluation of hot-wire measurements in wall shear turbulence using a direct numerical simulation database. Exp. Therm. Fluid Sci. 5, 69–77.

Temam, R., 1984. Navier–Stokes Equations, 3rd ed. North-Holland, Amsterdam.

Yabe, T., Aoki, T., 1991. A universal solver for hyperbolic equations by cubic-polynomial interpolation I. One-dimensional solver. Comp. Phys. Comm. 66, 219–232.

Zang, Y., Street, R.L., Koseff, J.R., 1994. A non-staggered grid, fractional step method for time-dependent incompressible Navier–Stokes equations in curvilinear coordinates. J. Comput. Phys. 114, 18–33.